*Inflammation, Vol. 40, No. 4, August 2017 (© 2017)*
DOI: 10.1007/s10753-017-0575-8

ORIGINAL ARTICLE

# JNK Inhibitor SP600125 Attenuates Paraquat-Induced Acute Lung Injury: an *In Vivo* and *In Vitro* Study

**Haitao Shen,[1] Na Wu,[2] Yu Wang,[1] Xinfei Han,[1] Qiang Zheng,[1] Xue Cai,[1] Honglei Zhang,[1] and Min Zhao[1,3]**

*Abstract*— Acute lung injury (ALI) is a major complication soon after paraquat poisoning and rapidly progresses with high mortality. However, the specific mechanism underlying paraquat-induced ALI is still unclear. In this study, the mechanism underlying the protective effects of SP600125 on paraquat-induced ALI was investigated according to oxidative stress, inflammation, and apoptosis. The rats were randomly assigned into the control group (CON), the paraquat poisoning group (PQ), and the PQ + SP600125 group (SP). A549 cells were divided into the Con group, Pq group, and Sp group. H&E staining and detection of lung wet/dry ratio were employed to evaluate lung injury. Annexin V-PI staining was done to evaluate A549 cell apoptosis. Dihydroethidium fluorescence was used to measure reactive oxygen species (ROS) in the lungs and A549 cells. ELISA was performed to detect TNF-α and IL-6 in the supernatant of broncho-alveolar lavage fluid (BALF) and A549 cells. RT-qPCR was done to measure the messenger RNA (mRNA) expression of TNF-α and IL-6 in the lungs and A549 cells. Western blotting assay was performed to detect the protein expression of phospho-JNK, total JNK, and cleaved caspase-3. Electrophoretic mobility shift assay was employed to detect the DNA binding activities of AP-1 and P-p65. JNK inhibitor SP600125 reduced JNK phosphorylation, downregulated cleaved caspase-3 protein level, decreased AP-1 transcriptional activity and ROS level, and reduced the transcription and expression of TNF-α and IL-6, which improved ALI and cell apoptosis after paraquat poisoning. Our results indicate that JNK/AP-1 mediates ALI as well as oxidative stress and inflammation deterioration secondary to paraquat poisoning.

**KEY WORDS:** acute lung injury; c-Jun N-terminal kinase; paraquat; apoptosis.

## INTRODUCTION

Paraquat poisoning is a fatal disease in clinical practice, and the associated mortality is as high as 30–70%. There is no specific antidote for paraquat poisoning [1]. Paraquat may enter the human body *via* the skin, respiratory tract, or gastrointestinal tract and then is distributed in the liver, kidney, and lungs. After it enters the human body, the paraquat concentration in the lungs is 10 times that of the blood. Acute lung injury (ALI) occurs soon after moderate to severe paraquat poisoning, often with a rapid progression and a variety of complications. Patients can quickly develop respiratory failure and multiple organ dysfunction or even die although active treatment is in progress [2].

Paraquat is a herbicide with a bipyridine structure that may block the intracellular electron transport chain [3],

[1] Department of Emergency Medicine, Shengjing Hospital of China Medical University, 36 Sanhao Street, Shenyang, 110004, People's Republic of China
[2] Department of Endocrinology, Shengjing Hospital of China Medical University, Shenyang, 110004, People's Republic of China
[3] To whom correspondence should be addressed at Department of Emergency Medicine, Shengjing Hospital of China Medical University, 36 Sanhao Street, Shenyang, 110004, People's Republic of China. E-mail: zhaom@sj-hospital.org

leading to the production of excess reactive oxygen species (ROS) and subsequent lipid peroxidation, which may directly rupture the cell membrane and kill the plant [4]. After entering the human body, paraquat may be transported into the liver *via* the polyamine transport system and then may accumulate in the lungs [5], causing a series of pathologic processes including cellular inflammation, calcium overload, and apoptosis [6]. Thus, ALI secondary to paraquat poisoning is the result of a cascade of events involving oxidative stress, inflammation, and apoptosis. c-Jun N-terminal kinase (JNK) is also known as stress-activated protein kinase and is an important member of the mitogen-activated protein kinase (MAPK) family. The JNK signaling pathway is involved in many physiopathologic processes and is closely related to apoptosis, inflammation, and oxidative stress [7]. Studies have shown that the JNK signaling pathway is involved in the pathogenesis of lung diseases [8]. Our previous study [9] showed that JNK in the lungs was activated after paraquat poisoning. However, the specific role of the JNK signaling pathway in paraquat poisoning, so here, we hypothesize that JNK activation exacerbates lung injury, and inhibition of JNK activation attenuates ALI induced by paraquat. In this study, a JNK inhibitor was used to treat rats and lung cells after paraquat poisoning, and the role of oxidative stress, inflammation, and apoptosis in the pathogenesis of ALI secondary to paraquat poisoning was further investigated.

## MATERIALS AND METHODS

### Materials

Paraquat standard, JNK inhibitor (SP600125), and MTT reagent (Sigma-Aldrich, St. Louis, MO, USA); dihydroethidium (DHE) (Santa Cruz Biotechnology, Santa Cruz, CA, USA); A549 cells (Chinese Academy of Sciences, Beijing, China); DMEM (Invitrogen, Carlsbad, CA, USA); fetal bovine serum (HyClone, Logan, UT, USA); tumor necrosis factor-α (TNF-α) and interleukin-6 (IL-6) ELISA kits (Boster, Wuhan, China); Annexin V-FITC Apoptosis Detection Kit and nuclear protein extraction kit (Beyotime, Haimen, China); JNK, p-JNK, cleaved caspase-3, and GAPDH antibodies (Santa Cruz Biotechnology, Santa Cruz, CA, USA); electrophoretic mobility shift assay (EMSA) kit (Viagene, Tampa, FL, USA); and AP-1 and P-p65 (p-p65) oligonucleotide probes (Beyotime, Haimen, China) were used in the present study.

### Animals and Establishment of Animal Model

A total of 36 specific pathogen-free male Sprague–Dawley rats weighing 200–250 g and aged 6–8 weeks were purchased from the Experimental Animal Center of the Affiliated Shengjing Hospital of China Medical University. Animals were housed at constant temperature (20–24 °C) and constant humidity (50–70%) with a 12/12-h light/dark cycle. Animals were given *ad libitum* access to food and water. The study was approved by the Ethics Committee of China Medical University (2015PS302K). Rats were allowed to accommodate to the environment for 5 days before experiments began. Then, animals were randomly divided into three groups: the normal control group (CON), the paraquat poisoning group (PQ), and the PQ + JNK inhibitor SP600125 group (SP) ($n$ = 12 per group). In the SP group, rats were intraperitoneally injected with 10 mg/mL SP600125 in DMSO at 15 mg/kg. In the PQ and CON groups, an equivalent volume of DMSO was intraperitoneally injected. One hour after injection, rats in the PQ and SP groups were intraperitoneally injected with 10 mg/mL paraquat in saline at 20 mg/kg. In the CON group, rats were intraperitoneally injected with an equal volume of normal saline. Our previous study confirmed that paraquat at 20 mg/kg caused poisoning in rats but was associated with a low mortality [10]. Thus, paraquat at 20 mg/kg was used in the present study.

### Sample Collection and Detection of Lung Wet/Dry Weight Ratio

At 72 h after the injection of paraquat or normal saline, rats were anesthetized and sacrificed. After disinfection, thoracotomy was performed, and the distal end of the trachea and the proximal end of the right main bronchus were ligated. A 1-mL syringe was used for lavage of the left lung *via* the trachea. The left lung was washed three times in triplicate, and the bronchoalveolar lavage fluid (BALF) was collected, followed by centrifugation at 3000 rpm for 10 min at 4 °C. The supernatant was collected and stored at −80 °C. The middle lobe of the right lung was collected and washed in normal saline. The water on the surface of the lung was removed, and the wet weight was obtained. Then, the lung tissues were placed in an oven at 80 °C. Then, 48 h later, the lungs were weighed again as the dry weight. The wet/dry weight ratio was calculated to evaluate lung edema: wet-to-dry (W/D) = wet weight (mg) / dry weight (mg). The remaining lung tissues were divided into two parts: one was fixed in 4% paraformaldehyde for further detection; the other was stored in liquid nitrogen and then at −80 °C for further detection.

### H&E Staining and Scoring of Lung Injury

Lung tissues were fixed in 4% paraformaldehyde, embedded in paraffin after dehydration, and sectioned, followed by H&E staining. The slide was treated with APES. Sections were deparaffinized, stained, dehydrated in ethanol, transparentized in xylene, and mounted. Then, sections were observed under a light microscope. Lung injury was scored as described by Mikawa *et al.* [11]: (1) alveolar congestion, (2) alveolar hemorrhage, and (3) infiltration or aggregation of neutrophils in the alveolar space or vascular wall, alveolar wall thickening, and/or hyaline membrane formation. These pathological features were independently scored using a five-point scale: 0 = no lesion or very mild lesion, 1 = mild lesion, 2 = moderate lesion, 3 = severe lesion, and 4 = very severe lesion. The sum of each score was the total score of lung injury (Fig. 1b, c).

### Cell Culture and Establishment of a Cell Model

A549 cells were maintained in DMEM containing 10% fetal bovine serum at 37 °C with 5% $CO_2$. The medium was refreshed once every 2 days. When cell confluence reached 60–70%, cells were digested with 0.25% trypsin and passaged at a ratio of 1:3. Cells in the logarithmic growth phase were used in subsequent experiments. A549 cells were seeded into 96-well plates at a density of $1 \times 10^4$/well. Cells were divided into the blank control group (cells were maintained in DMEM), the normal control group (cells were not treated with paraquat), and different paraquat groups (cells were treated with paraquat at different concentrations 100, 200, 400, 600, 800, 1000, and 1200 μM) ($n$ = 4 wells/group). Cells were maintained at 37 °C for 72 h to determine the optimal concentration of paraquat. MTT solution (20 μL) was added to each well at the end of treatment, followed by incubation at 37 °C for 4 h. The supernatant was removed, and DMSO (150 μL) was added to each well to resolve the crystals within 10 min. Absorbance (A) was measured at 560 nm. Cell viability (%) was calculated using the equation:

$$\text{Cell viability}\ (\%) = \left(A_{\text{paraquat}} - A_{\text{blank control}}\right) / \left(A_{\text{normal control}} - A_{\text{blank control}}\right) \times 100\%$$

In subsequent experiments, the authors used the concentration of paraquat at which the cell viability was close to

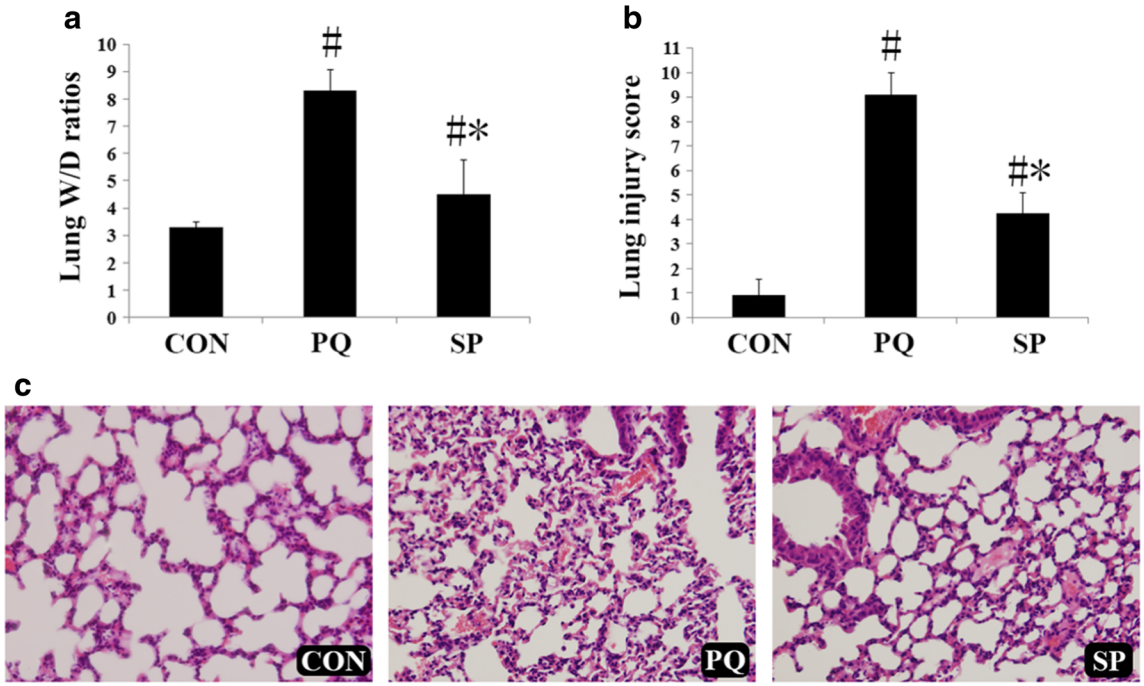


**Fig. 1.** SP reduces the W/D ratio and attenuates lung injury in rats after paraquat poisoning. **a** Lung W/D ratios of rats in different groups. **b** Lung injury score of rats in different groups. **c** H&E staining of the lungs in different groups. *CON* the control group, *PQ* the paraquat poisoning group, *SP* the JNK inhibitor SP600125 treatment group. Data are means ± SDs. $n$ = 12/group. #$p < 0.05$ *vs.* CON; *$p < 0.05$ *vs.* PQ.

50%. Cells were then divided into the Con group, the Pq group, and the JNK inhibitor SP600125 group (Sp). Cells in each group were seeded into 6-well plates at a density of $2 \times 10^5$/well. In the Sp group, cells were treated with 50 μM SP600125 for 24 h. Cells in the Pq group and the Sp group were treated with paraquat at the concentration determined above. In the Con group, cells were treated with an equal volume of PBS. After paraquat treatment for 72 h, the medium was removed and DHE solution was added, followed by incubation at 37 °C for 45 min. Then, cells were observed under a fluorescence microscope. ROS-positive cells presented red fluorescence in the nucleus.

### Detection of Apoptosis by Annexin V-PI Staining

Cells in each group were seeded into 6-well plates. Cells were digested with trypsin before detection, followed by centrifugation at 1000 rpm. The supernatant was removed, and cells were rinsed twice in PBS (10 min for each rinse). Then, cells were resuspended in 400 μL of binding buffer, followed by the addition of 5 μL of Annexin V-FITC. After incubation at room temperature for 15 min, 5 μL of propidium iodide (PI) was added, followed by incubation for another 5 min. After addition of 100 μL of buffer, cells were subjected to flow cytometry with an excitation wavelength of 488 nm. Annexin V-FITC was detected *via* the FL1 channel and PI *via* the FL2 channel. Analysis was done with CellQuest software (BD Bioscience, San Jose, CA, USA).

### Detection of TNF-α and IL-6 by ELISA

At the end of treatment, the medium was removed, cells were centrifuged at 10,000 rpm for 10 min, and the supernatant was collected. The concentrations of TNF-α and IL-6 were measured according to the manufacturer's instructions. The serum contents of TNF-α and IL-6 were also measured by ELISA.

### Detection of ROS by DHE Staining

Lung tissues stored at −80 °C were processed as previously reported [12]. Cells were seeded onto glass coverslips for the DHE staining: Tissues were embedded in OCT and then sectioned. Lung sections on the slides and A549 cells on the coverslips were stained with DHE solution at 37 °C for 30 min. DHE is oxidized and embedded into DNA, showing red fluorescence. Samples were then observed under a fluorescence microscope (BX41, Olympus, Tokyo, Japan). Representative images were captured, and fluorescence intensity was determined with Image Pro Plus 6.0.

### Detection of TNF-α and IL-6 mRNA expression by RT-qPCR

Cells were seeded into 6-well plates and harvested for the extraction of total RNA using the Qiagen RNeasy kit (Valencia, CA, USA). RNA was then reversely transcribed into cDNA with an Applied Biosystems TaqMan kit (Foster City, CA, USA), followed by RT-qPCR with a thermal cycler for the detection of TNF-α and IL-6 messenger RNA (mRNA) expression. The lung tissues were collected, and total RNA was extracted. RT-qPCR was also performed to detect the TNF-α and IL-6 mRNA expression.

The primers used for RT-qPCR of cDNA from A549 cells were as follows:

TNF-α forward primer 5′-CCTCTCTCTAATCAGCCC TCTG-3′ and reverse primer 5′-GAGGACCT GGGAGTAGATGAG-3′.
IL-6 forward primer 5′-ACTCACCTCTTCAGAACG AATTG-3′ and reverse primer 5′-CCATCTTT GGAAGGTTCAGGTTG-3′.
β-Actin forward primer 5′-ATGCTCCC CGGGCTGTAT-3′ and reverse primer 5′-CATAGGAG TCCTTCTGACCCATT-3′.

The primers used for RT-qPCR of cDNA from lung tissues were as follows:

IL-6 forward primer 5′-CACTTCACAAGTCGGAGG CT-3′ and reverse primer 5′-AGCACACT AGGTTTGCCGAG-3′.
TNF-α forward primer 5′-GATCGGTC CCAACAAGGAGG-3′ and reverse primer 5′-CTCC CTCAGGGGTGTCCTTA-3′.
β-Actin forward primer 5′-GTGGATCA GCAAGCAGGAGT-3′ and reverse primer 5′-CGCA GCTCAGTAACAGTCCG-3′.

### Detection of Protein Expression by Western Blotting

The protein expressions of p-JNK, total JNK, and cleaved caspase-3 were detected by Western blotting assays. In brief, lung tissues and cells were independently treated with lysis buffer, followed by extraction of total protein. In addition, lung tissues and cells were also subjected to extraction of membrane proteins, nuclear proteins, and cytoplasmic proteins. After quantification of protein concentration using the BCA method, proteins were boiled in loading buffer for 5 min. Then, 20 μL of total proteins were subjected to 10% SDS-PAGE at 150 V and 30 mA for 1.5 h and then were transferred onto PVDF membrane at 50 V for 2 h. The membrane was blocked in 5% nonfat

milk, followed by incubation with primary antibodies at 4 °C overnight. The primary antibodies against the following proteins were used: p-JNK, JNK, cleaved caspase-3 (only cell), and GAPDH for total proteins. After washing in TBST thrice (5 min for each), the membrane was incubated with secondary antibody (1:500) for 2 h at room temperature. After washing in 0.1% TBST thrice (15 min for each wash), visualization was done with enhanced chemiluminescence (ECL); the optical density was measured with Gel-Pro Analyzer 3.0 (Vendor, City, Country).

### Detection of AP-1 and P-p65 DNA Binding Activity by EMSA

Nuclear proteins were incubated with a biotinylated oligonucleotide probe at room temperature for 15 min. The sequence of the universal oligonucleotide probe was 5′-CGC TTG ATG ACT CAG CCG GAA-3′ for AP-1 and 5′-AGT TGA GGG GAC TTT CCC AGG C-3′ for P-p65. After 6% nondenaturing PAGE for 60 min and transferring for 20 min, the DNA–protein interaction was done by UV cross-linking. After addition of streptavidin-HRP, visualization was done with ECL, and the optical density was measured with Gel-Pro Analyzer 3.0 (Vendor, City, Country).

### Statistical Analysis

Data were expressed as means ± standard deviations (SD). Statistical analysis was performed with SPSS 17.0 (IBM, Armonk, NY, USA). Comparisons were done with one-way analysis of variance (ANOVA) among groups and with the *t* test for comparisons between two groups. A value of $p < 0.05$ was considered statistically significant.

## RESULTS

### SP Reduces Lung W/D Ratio and Attenuates Lung Injury

When compared with that of the CON group, the W/D ratio increased significantly in the PQ group. After JNK inhibitor pretreatment, the W/D ratio was reduced markedly compared with that of the PQ group (Fig. 1a). In the CON group, the alveolar structure was clear, and the alveolar wall was thin; there was no thickening and congestion of the alveolar septum, and infiltration of inflammatory cells and hemorrhage were not observed. At 72 h after paraquat injection, the alveolar structures were significantly damaged, edema was present in the lung interstitium and alveoli, the alveolar space was collapsed, and bloody fluid and red blood cells appeared in some alveolar spaces. There was infiltration of neutrophils and macrophages, and hyaline membrane formation was noted in some alveolar spaces. In the presence of SP pretreatment, lung hemorrhage and lung edema were significantly improved (Fig. 1c). In the PQ group, the lung injury score increased significantly compared with that of the CON group, but SP pretreatment markedly reduced the lung injury score compared to that of the PQ group (Fig. 1b).

### SP Reduces ROS and mRNA Expression of TNF-α and IL-6 in the Lungs of Rats After Paraquat Poisoning

The red fluorescence intensity can reflect the ROS level in the lungs. DHE staining showed that the ROS level in the lungs increased significantly after paraquat poisoning in rats, but SP pretreatment markedly reduced the ROS levels in the lungs (Fig. 2a). RT-qPCR indicated that the mRNA expression of TNF-α and IL-6 in the lungs increased significantly after paraquat poisoning, but SP pretreatment markedly reduced the mRNA expression of TNF-α and IL-6 in the lungs (Fig. 2b).

### SP Reduces JNK Phosphorylation and Inhibits AP-1 DNA Binding Activity but Has No Influence on P-p65 DNA Binding Activity in Rats

Western blotting assays showed that the protein levels of p-JNK in the lung significantly increased after paraquat poisoning compared with the protein expression in the CON group, but SP pretreatment significantly reduced the protein levels of p-JNK compared with that in the PQ group (Fig. 3a). EMSA indicated that the AP-1 DNA binding activity and the p-p65 DNA binding activity in the lung increased significantly after paraquat poisoning; SP pretreatment markedly reduced AP-1 DNA binding activity but failed to markedly reduce the P-p65 DNA binding activity (Fig. 3b, c).

### PQ Affects the Viability of A549 Cells in a Dose-Dependent Manner

Cells were treated with paraquat at 100, 200, 400, 600, 800, 1000, and 1200 μmol/L for 72 h, and MTT assay showed that the cell viability was reduced to 78.20, 68.07, 51.94, 47.37, 41.85, 25.40, and 10.12%, respectively. This indicates that PQ may affect the viability of A549 cells in a dose-dependent manner: The higher the dose of paraquat, the lower the viability. When the paraquat concentration was 400 μmol/L, the cell viability was 51.94%, which was

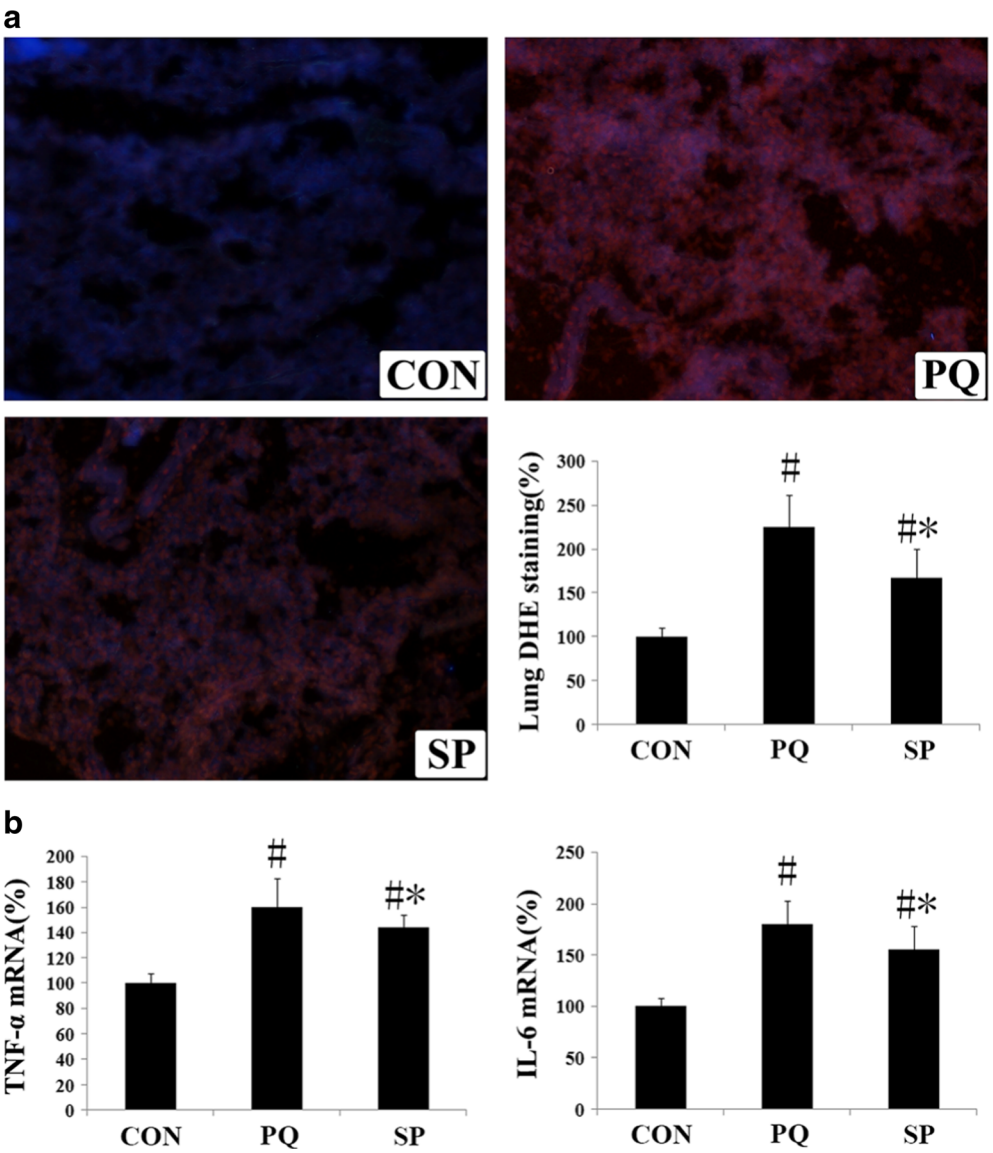


**Fig. 2.** SP reduces ROS and mRNA expression of inflammatory cytokines in the lungs after paraquat poisoning. **a** Dihydroethidium (DHE) staining of the lungs in different groups and DHE fluorescence intensity of the lungs in different groups. **b** TNF-α and IL-6 mRNA expression in the lungs (RT-qPCR). *CON* the control group, *PQ* the paraquat poisoning group, *SP* the JNK inhibitor SP600125 treatment group. Data are means ± SDs. $n = 12$/group. #$p < 0.05$ *vs.* CON; *$p < 0.05$ *vs.* PQ.

closest to the target of approximately 50% (Fig. 4). Thus, paraquat at 400 μmol/L was used in subsequent experiments.

### SP Reduces Apoptotic Cells After Paraquat Poisoning

Flow cytometry showed that the apoptosis rate was the lowest in the Con group and increased significantly after paraquat poisoning, but SP pretreatment markedly reduced the apoptosis rate (Fig. 5).

### SP Reduces ROS Level and mRNA Expression of TNF-α and IL-6 in A549 Cells After Paraquat Poisoning

DHE staining showed that the ROS level in A549 cells increased significantly after paraquat poisoning,

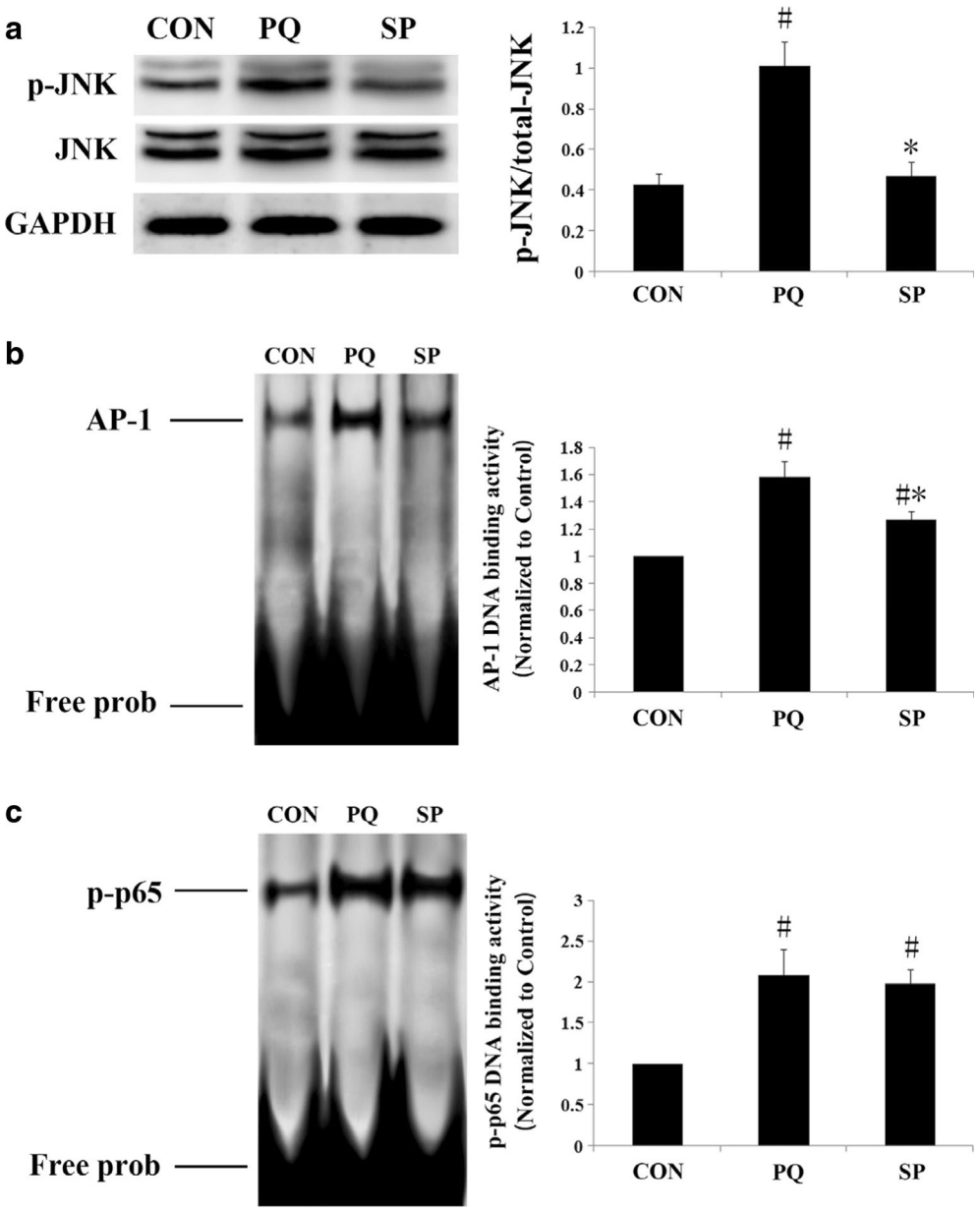


**Fig. 3.** SP reduces JNK phosphorylation and AP-1 DNA binding activity in the lungs but has no influence on NF-κB phospho-p65 DNA binding activity. **a** c-Jun N-terminal kinase (JNK) and p-JNK expression in the lungs of different groups (Western blotting). **b** Activator protein-1 (AP-1) DNA binding activity (EMSA). **c** Phospho-p65 DNA binding activity (EMSA). *CON* the control group, *PQ* the paraquat poisoning group, *SP* the JNK inhibitor SP600125 treatment group. Data are means ± SDs. $n = 12$/group. #$p < 0.05$ *vs.* CON; *$p < 0.05$ *vs.* PQ.

but SP pretreatment markedly reduced the ROS level after paraquat poisoning (Fig. 6a). RT-qPCR showed that the mRNA expression of TNF-α and IL-6 in A549 cells increased significantly after paraquat poisoning compared with expression in the CON group, but SP pretreatment markedly reduced the mRNA expression of TNF-α and IL-6 in A549 cells compared with that in the PQ group (Fig. 6b).

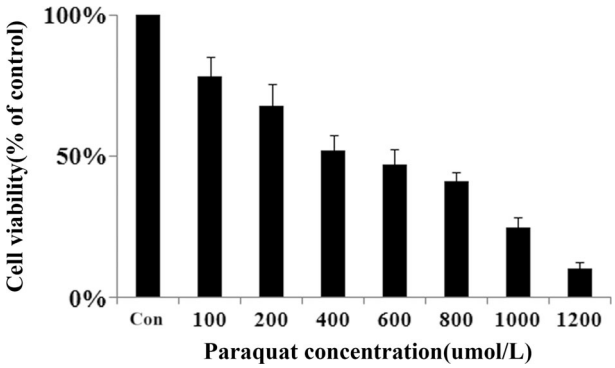


**Fig. 4.** PQ affects the viability of A549 cells in a dose-dependent manner. A549 cells were treated with paraquat at 100, 200, 400, 600, 800, 1000, and 1200 μmol/L for 72 h, and the MTT assay was performed to detect cell viability. Data are means ± SDs. $n = 5$/group.

### SP Reduces p-JNK and Cleaved Caspase-3 Protein Levels and Inhibits AP-1 and P-p65 DNA Binding Activity *In Vitro*

Western blotting assays showed that the protein levels of p-JNK and cleaved caspase-3 in A549 cells significantly increased after paraquat poisoning compared with the protein expression in the Con group, but SP pretreatment significantly reduced the protein levels of p-JNK and cleaved caspase-3 compared with that in the Pq group (Fig. 7a, b). EMSA indicated that the AP-1 DNA binding activity and the p-p65 DNA binding activity in A549 cells increased markedly after paraquat poisoning, and SP pretreatment reduced the AP-1 DNA binding activity and the p-p65 DNA binding activity (Fig. 7c, d).

### SP Reduces the Levels of Inflammatory Cytokines in the Supernatant and BALF

ELISA showed that the levels of TNF-α and IL-6 in the BALF increased significantly compared with those in the CON group, but SP pretreatment markedly reduced the contents of TNF-α and IL-6 in the BALF (Fig. 8a, b). After paraquat poisoning, the levels of TNF-α and IL-6 in the supernatant increased markedly after paraquat poisoning compared with the levels in the Con group, but SP pretreatment reduced the levels of TNF-α and IL-6 in the supernatant of A549 cells (Fig. 8c, d).

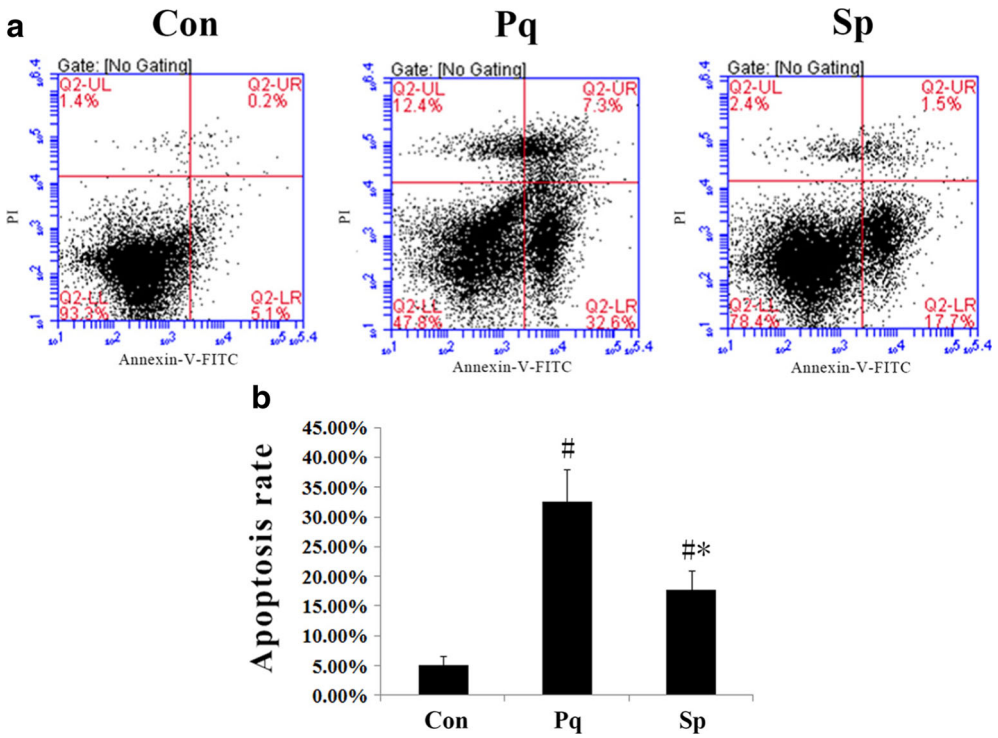


**Fig. 5.** SP reduces the apoptosis rate of A549 cells after paraquat poisoning. **a** Detection of apoptosis by Annexin V-PI staining. **b** Apoptosis rate. *Con* the control group, *Pq* the paraquat poisoning group, *Sp* the JNK inhibitor SP600125 treatment group. Data are means ± SDs. $n = 5$/group. #$p < 0.05$ *vs.* Con; *$p < 0.05$ *vs.* Pq.

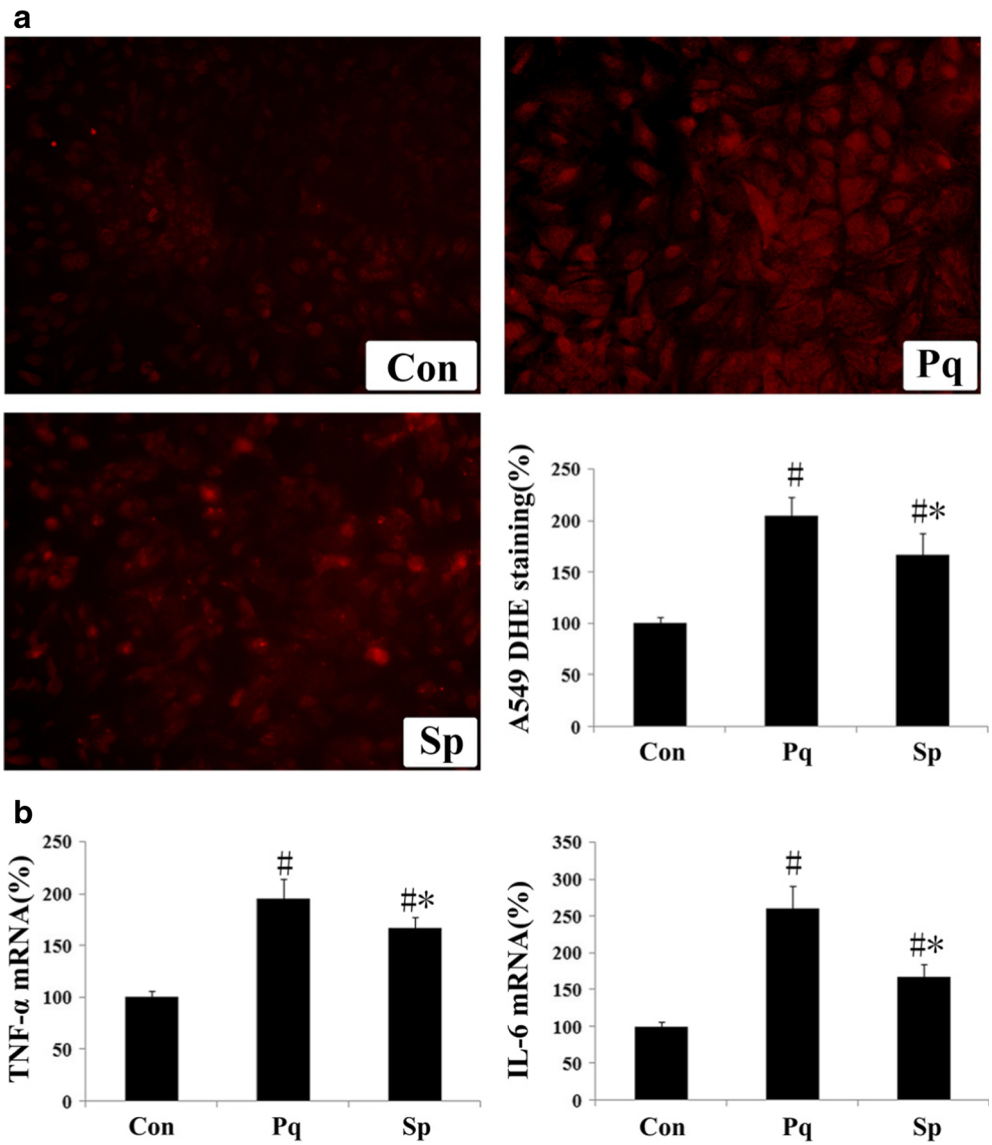


**Fig. 6.** SP reduces ROS and inflammatory cytokine transcription in A549 cells after paraquat poisoning. **a** Detection of ROS in cells by DHE staining. **b** TNF-α and IL-6 mRNA expression in the supernatant of A549 cells (RT-qPCR). *Con* the control group, *Pq* the paraquat poisoning group, *Sp* the JNK inhibitor SP600125 treatment group. Data are means ± SDs. $n = 5$/group. #$p < 0.05$ *vs.* Con; *$p < 0.05$ *vs.* Pq.

## DISCUSSION

Fatal paraquat poisoning usually causes obvious pathological changes within 48 h [13]. Our previous study [9] showed evident lung injury and JNK activation within 48–72 h after paraquat poisoning. Thus, detections were done at 72 h after paraquat poisoning, and the study also revealed typical ALI at this time. In the present study, our results showed that a JNK-specific inhibitor attenuated ALI and A549 cell apoptosis after paraquat poisoning, accompanied by reductions in inflammatory cytokines and oxidative stress. This indicates that paraquat poisoning-induced ALI is mediated by the JNK/AP-1 signaling pathway, and interventions targeting this pathway may provide options for the treatment of paraquat poisoning. These findings also indicate a direction for the management of critical illnesses characterized by uncontrollable release of inflammatory cytokines and excessive

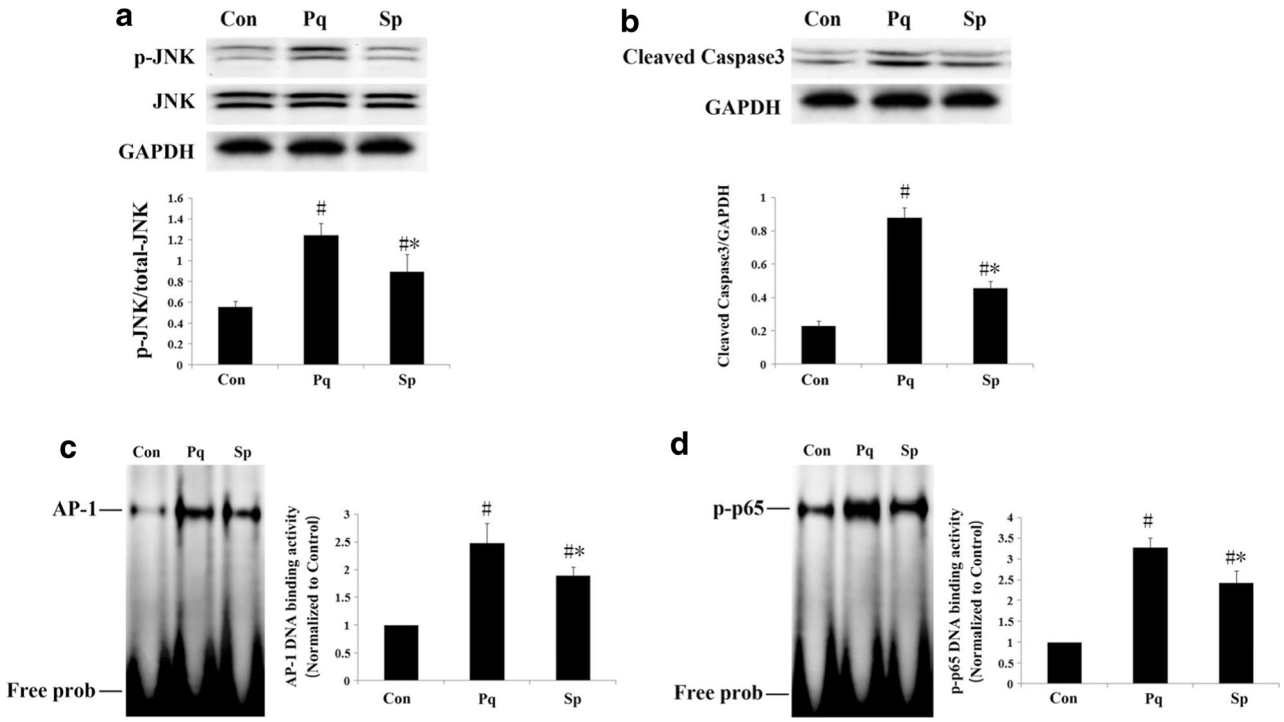


**Fig. 7.** SP decreases the p-JNK and cleaved caspase-3 level and reduces AP-1, NF-κB, and phospho-p65 DNA binding activity *in vitro*. **a** JNK protein expression in A549 cells (Western blotting). **b** Cleaved caspase-3 protein expression in A549 cells (Western blotting). **c** AP-1 DNA binding activity (EMSA). **d** Phospho-p65 DNA binding activity (EMSA). *Con* the control group, *Pq* the paraquat poisoning group, *Sp* the JNK inhibitor SP600125 treatment group. Data are means ± SDs. $n = 5$/group. #$p < 0.05$ *vs.* Con; *$p < 0.05$ *vs.* Pq.

oxidative stress (such as systemic inflammatory response syndrome and multiple organ dysfunction syndrome).

The MAPK family mainly includes JNK, ERK, and p38, of which the MAPK and ERK signaling pathways have been confirmed to attenuate ALI secondary to paraquat poisoning [14–16], and *in vitro* experiments also confirm these results [17]. These findings suggest that the MAPK family plays an important role in the pathogenesis of ALI after paraquat poisoning, but the role of JNK, an important member of the MAPK family, in ALI after paraquat poisoning has never been investigated. JNK can be activated by multiple factors, including cytokines (such as TNF-α and EGF) and stress (such as UV and oxidative injury) [18]. Activated JNK then regulates the expression of downstream target genes or the activity of downstream target proteins, leading to pathologic processes that include inflammation and apoptosis. The AP-1 complex is an important substrate of JNK and is composed of c-jun and c-fos. Activated AP-1

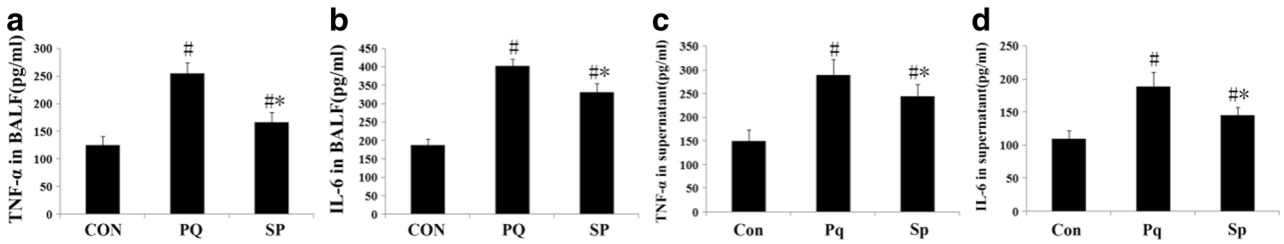


**Fig. 8.** SP reduces inflammatory cytokines in the BALF of rats and in the supernatant of A549 cells after paraquat poisoning. **a** TNF-α content in the BALF of rats (ELISA). **b** IL-6 content in the BALF of rats (ELISA). *CON* the control group, *PQ* the paraquat poisoning group, *SP* the JNK inhibitor SP600125 treatment group. Data are means ± SDs. $n = 12$/group. #$p < 0.05$ *vs.* CON; *$p < 0.05$ *vs.* PQ. **c** TNF-α content in the supernatant of A549 cells (ELISA). **d** IL-6 content in the supernatant of A549 cells (ELISA). *Con* the control group, *Pq* the paraquat poisoning group, *Sp* the JNK inhibitor SP600125 treatment group. Data are means ± SDs. $n = 5$/group. #$p < 0.05$ *vs.* Con; *$p < 0.05$ *vs.* Pq.

enters the nucleus and then binds to DNA to regulate the expression of certain cytokines such as IL-6 and TNF-α [19]. In the present study, paraquat poisoning significantly increased JNK activation (p-JNK), which enhanced AP-1 and p-p65 DNA binding activity and expression of IL-6 and TNF-α, accompanied by evident lung injury and cell apoptosis. In a paraquat poisoning model, Cho *et al*. [20] detected the expression of 1120 proteins and found that the expression of JNK-related molecules increased after paraquat poisoning. This indicates that the JNK signaling pathway is activated during paraquat poisoning. To investigate the role of JNK in ALI secondary to paraquat poisoning, a JNK inhibitor was used. JNK has three subtypes: JNK1, JNK2, and JNK3, of which JNK1/2 is widely expressed in the human body, and JNK3 is expressed only in the nervous system, heart, and testis [21]. Thus, a JNK1/2-specific inhibitor SP600125 was used in this study to inhibit JNK1/2 phosphorylation [22].

Although some studies show that JNK signaling is involved in pro-inflammation [23], it may interact at different levels, which indicates that JNK activation induced by different stimuli may result in distinct outcomes [24]. Evidence shows that JNK mediates lipopolysaccharide-induced NF-κB activation [25]. However, in dieckol-induced antihepatic fibrosis, the change in JNK was opposite than that in NF-κB [26]. Meyer *et al*. also found that, in the presence of a potent antioxidant, JNK can inhibit the DNA binding activity of p-p65 in the nucleus [27]. In the present study, paraquat poisoning activated the JNK signaling pathway, and AP-1 and NF-κB were also activated. In the presence of a JNK inhibitor, AP-1 DNA binding activity was significantly reduced, and it was interesting for NF-κB DNA binding activity that it showed significant reducing *in vitro* but was only slightly reduced *in vivo*; this indicates that NF-κB activation after paraquat poisoning does not depend on the JNK signaling pathway in some other lung cells except type II alveolar epithelial cell. In addition, the expression of IL-6 and TNF-α, which is downstream factors of JNK, was reduced significantly in the presence of the JNK inhibitor, which was accompanied by the attenuation of ALI. This implies that ALI and the release of inflammatory cytokines after paraquat poisoning are mediated mainly by JNK/AP-1.

Oxidative stress refers to the accumulation of ROS due to imbalance between ROS clearance and generation. Almost all pathologic factors may cause excess production of ROS or compromise the clearance of ROS, which disrupts the balance between ROS generation and ROS clearance, thereby leading to an increase in ROS and oxidative stress [28, 29]. ROS includes the superoxide anion ($O_2^-$), hydrogen peroxide ($H_2O_2$), and hydroxyl radicals (·OH). In the present study, a superoxide-labeled fluorescent probe (DHE) was used to detect ROS in the lung tissues and A549 cells. This dye may enter the cells, where it can be oxidized into ethidium bromide in the presence of superoxide, and then, ethidium bromide binds to DNA and produces red fluorescence. The fluorescence intensity reflects the amount of ROS generated in cells and represents the level of oxidative stress. Paraquat is an electron acceptor, and thus, the uncontrollable production of ROS is an early consequence of paraquat poisoning [30]. ROS may act on the apoptosis signal-regulated kinase pathway [31] and the Src protein pathway to activate the JNK signaling pathway [32]. However, this activity is not unidirectional. Wajant *et al*. found interactions between JNK and ROS [33]. In human U937 cells, the JNK pathway may activate caspase-3 to upregulate ROS [34]. In the present study, JNK activation induced caspase-3 activation and upregulated ROS, suggesting positive feedback between ROS and JNK after paraquat poisoning, and JNK blockade also reduced ROS. Thus, it remains for an elegantly designed study to elucidate the specific mechanisms and to provide new insights for the management of uncontrollable oxidative stress secondary to paraquat poisoning. But our study just aims on inhibition of JNK phosphorylation without the genetic intervention, and pulmonary fibrosis following paraquat poisoning was not investigated in the present study either, so complex and further studies should be done in this field.

## CONCLUSION

*In vitro* and *in vivo* studies show that paraquat poisoning may activate the JNK/AP-1 pathway to increase the release and expression of TNF-α and IL-6 and thereby to increase oxidative stress, leading to ALI and A549 cell apoptosis. Inhibition of JNK with a specific inhibitor may inhibit AP-1 activation, attenuate oxidative stress, and downregulate the expression and release of TNF-α and IL-6, thereby alleviating ALI and A549 cell apoptosis.

## COMPLIANCE WITH ETHICAL STANDARDS

**Conflict of Interest.** The authors declare that they have no conflict of interest.

**Funding.** This study was funded by Science Foundation of Liaoning Education Department (grant numbers LK201633 and LK201603), Peking Union Medical Foundation-Ruiyi Emergency Medical Research Fund (grant number R2015021), and Provincial Natural Science Foundation of Liaoning (grant number 201602879).

## REFERENCES

1. Dinisoliveira, R.J., J.A. Duarte, A. Sáncheznavarro, et al. 2008. Paraquat poisonings: mechanisms of lung toxicity, clinical features, and treatment, critical Reviews in Toxicology. *Informa Healthcare. Critical Reviews in Toxicology* 38 (1): 13.
2. Gawarammana, I.B., and N.A. Buckley. 2011. Medical management of paraquat ingestion. *British Journal of Clinical Pharmacology* 72 (5): 745–757.
3. Slade, P. 2006. The fate of paraquat applied to plants. *Weed Research* 6 (2): 158–167.
4. Dodge, A.D. 1971. The mode of action of bipyridylium herbicides, paraquat and diquat. *Endeavour* 30 (111): 130.
5. Hoet, P.H., C.P. Lewis, M. Demedts, et al. 1994. Putrescine and paraquat uptake in human lung slices and isolated type II pneumocytes. *Biochemical Pharmacology* 48 (3): 517–524.
6. Bird, C.L., and A.T. Kuhn. 1981. Electrochemistry of the viologens. *Chemical Society Reviews* 10 (1): 49–82.
7. Rd, R.J., S. Horowitz, W.R. Franek, et al. 2003. MAPK pathways mediate hyperoxia-induced oncotic cell death in lung epithelial cells. *Free Radical Biology & Medicine* 35 (8): 978–993.
8. Kim, Y.R., I.K. Kim, S.H. Seo, et al. 2010. Effect of toluene on RANTES and eotaxin expression through the p38 and JNK pathways in human lung epithelial cells. *Molecular & Cellular Toxicology* 6 (4): 344–350.
9. Liu, Z., Y. Wang, H. Zhao, et al. 2013. CB2 receptor activation ameliorates the proinflammatory activity in acute lung injury induced by paraquat. *BioMed Research International* 2014 (2): 971750.
10. Liu, Z., M. Zhao, Q. Zheng, et al. 2013. Inhibitory effects of rosiglitazone on paraquat-induced acute lung injury in rats. *Acta Pharmacologica Sinica* 34 (10): 1317–1324.
11. Mikawa, K., K. Nishina, Y. Takao, et al. 2003. ONO-1714, a nitric oxide synthase inhibitor, attenuates endotoxin-induced acute lung injury in rabbits. *Anesthesia & Analgesia* 97 (6): 1751–1755.
12. Wu, N., H. Shen, H. Liu, et al. 2016. Acute blood glucose fluctuation enhances rat aorta endothelial cell apoptosis, oxidative stress and pro-inflammatory cytokine expression in vivo. *Cardiovascular Diabetology* 15 (1): 109.
13. Mohammadi-Bardbori, A., and M. Ghazi-Khansari. 2008. Alternative electron acceptors: proposed mechanism of paraquat mitochondrial toxicity. *Environmental Toxicology and Pharmacology* 26 (1): 1–5.
14. Raman, M., W. Chen, and M.H. Cobb. 2007. Differential regulation and properties of MAPKs. *Oncogene* 26 (22): 3100.
15. Pei, Y.H., X.M. Cai, J. Chen, et al. 2014. The role of p38 MAPK in acute paraquat-induced lung injury in rats. *Inhalation Toxicology* 26 (14): 880.
16. Seo, H.J., S.J. Choi, and J.H. Lee. 2014. Paraquat induces apoptosis through cytochrome C release and ERK activation. *Biomolecules & Therapeutics* 22 (6): 503.
17. Huang, M., Y.P. Wang, L.Q. Zhu, et al. 2015. MAPK pathway mediates epithelial-mesenchymal transition induced by paraquat in alveolar epithelial cells. *Environmental Toxicology* 31 (11): 1407–1414.
18. Nakamura, G.L.J.K. 2007. The c-Jun kinase/stress-activated pathway: regulation, function and role in human disease. *Biochimica et Biophysica Acta* 1773 (8): 1341–1348.
19. Sabapathy, K. 2012. Role of the JNK pathway in human diseases. *Progress in Molecular Biology & Translational Science* 106: 145.
20. Cho, I.K., M. Jeong, A.S. You, et al. 2015. Pulmonary proteome and protein networks in response to the herbicide Paraquat in rats. *Journal of Proteomics & Bioinformatics* 08 (5): 67–79.
21. Davies, C., and C. Tournier. 2012. Exploring the function of the JNK (c-Jun N-terminal kinase) signalling pathway in physiological and pathological processes to design novel therapeutic strategies. *Biochemical Society Transactions* 40 (1): 85.
22. Bogoyevitch, M.A., and P.G. Arthur. 2015. Inhibitors of c-Jun N-terminal kinases: JuNK no more? *Biochimica et Biophysica Acta* 58 (1): 72–95.
23. Davis, R.J. 2000. Signal transduction by the JNK group of MAP kinases. *Cell* 103 (2): 239.
24. Repici, M., R. Wehrlé, X. Antoniou, et al. 2011. C-Jun N-terminal kinase (JNK) and p38 play different roles in age-related Purkinje cell death in murine organotypic culture. *The Cerebellum* 10 (2): 281–290.
25. Hui, S.L., H.J. Kim, S.M. Chang, et al. 2004. Inhibition of c-Jun NH 2-terminal kinase or extracellular signal-regulated kinase improves lung injury. *Respiratory Research* 5 (1): 23.
26. LeeS, LeeJ, LeeH, et al(2016) MicroRNA134 mediated upregulation of JNK and downregulation of NFkB signalings are critically involved in Dieckol induced antihepatic fibrosis. J Agric Food Chem64(27).
27. Meyer, M., R. Schreck, and P.A. Baeuerle. 1993. H2O2 and antioxidants have opposite effects on activation of NF-kappa B and AP-1 in intact cells: AP-1 as secondary antioxidant-responsive factor. *EMBO Journal* 12 (5): 2005.
28. Apel, K., and H. Hirt. 2004. Reactive oxygen species: metabolism, oxidative stress, and signal transduction. *Annual Review of Plant Biology* 55: 373–399.
29. Finkel, T., and N.J. Holbrook. 2000. Oxidants, oxidative stress and the biology of ageing. *Nature* 408 (6809): 239–247.
30. Montgomery, M.R., and D.E. Niewoehner. 1979. Oxidant-induced alterations in pulmonary microsomal mixed-function oxidation: acute effects of paraquat and ozone. *Journal of Environmental Science & Health Part C Environmental Health Sciences* 13 (3): 205–219.
31. Nagai, H., T. Noguchi, K. Takeda, et al. 2007. Pathophysiological roles of ASK1-MAP kinase signaling pathways. *Journal of Biochemistry & Molecular Biology* 40 (1): 1–6.
32. Chen, K., J.A. Vita, B.C. Berk, et al. 2001. C-Jun N-terminal kinase activation by hydrogen peroxide in endothelial cells involves Src-dependent epidermal growth factor receptor transactivation. *Journal of Biological Chemistry* 276 (19): 16045.
33. Wajant, H., K. Pfizenmaier, and P. Scheurich. 2003. Tumor necrosis factor signaling. *Cell Death and Differentiation* 10: 45–65.
34. Kim, E.M., H.S. Yang, S.W. Kang, et al. 2008. Amplification of the γ-irradiation-induced cell death pathway by reactive oxygen species in human U937 cells. *Cellular Signalling* 20 (5): 916–924.